Eur. Phys. J. B **7**, 563–572 (1999)

THE EUROPEAN PHYSICAL JOURNAL B

EDP Sciences

An attempt to model the dielectric function in II-VI ternary compounds $Hg_{1-x}Zn_xTe$ and $Cd_{1-x}Zn_xTe$

O. Castaing, J.T. Benhlal, and R. Granger

Laboratoire de Physique des Solides, INSA, CS 14315, 35043 Rennes Cedex, France

Received: 22 May 1998 / Revised: 21 September 1998 / Accepted: 28 September 1998

Abstract. The dielectric function ε of II-VI ternaries is described by fitting experimental results at room temperature to three different models. For each individual composition, ε variations with photon energy E are well reproduced with only four harmonic oscillators. The model dielectric function (MDF) of Adachi which is linked to the band structure does not give better results in the description of $\varepsilon(E)$ and its derivatives are not correctly reproduced. The MDF model of Kim *et al.* lead to good descriptions both of $\varepsilon(E)$ and its derivatives in all the spectral range considered, and it appears the most powerful model at the present time. We have not fully succeeded in building a composition dependent model for these bulk semiconductors. The analysis of this failure reveals that, though the materials appear good, their unknown densities of defects appear uncorrelated with the composition of the ternaries. These non controlled defect densities lead mainly to erratic deviations of the broadenings near critical transitions. Though relatively small these erratic deviations on the broadenings prevent the set up of a precise composition dependent model. $\varepsilon(E)$ variations are also calculated below the fundamental gap in HgZnTe and CdZnTe. Zero frequency (ε_∞) values are compared with known experimental results. The large variation of ε_∞ with composition x in $Hg_{1-x}Zn_xTe$ prevents the revealing of the part of ε due to the defects. In return, the effect of the defects on the crystal polarizability is evidenced in $Cd_{1-x}Zn_xTe$ where the variation of ε_∞ with x is small. This leads us to propose that the most probable values of ε_∞ are near 7.1 for CdTe and 6.75 for ZnTe.

PACS. 78.20.-e Optical properties of bulk materials and thin films – 71.22.+i Electronic structure of liquid metals and semiconductors and their alloys – 77.22.Ch Permittivity (dielectric function)

1 Introduction

Modeling the optical dielectric function is of paramount importance for the design of optoelectronic devices [1]. The dielectric function of a material $\varepsilon(E) = \varepsilon_r(E) + i\varepsilon_i(E)$, where E is the photon energy, can be measured using spectroscopic ellipsometry. These measurements are usually performed at room temperature for semiconductors. $\varepsilon(E)$ has been measured at low temperatures only for a limited number of semiconductors such as Si [2], Ge, GaAs [3], InSb or InP [4]. For ternary and quaternary compounds, $\varepsilon(E)$ is only known for a limited number of compositions. In this paper $\varepsilon(E)$ will designate experimental determinations of the dielectric function and $L(E) = L_r(E) + iL_i(E)$ its values deduced from models. Several linear schemes have been proposed to evaluate $L(E)$ for any composition. They are based on purely mathematical grounds [5,6] or use the effective medium approximation [7]. All these schemes need the tabulated values of $\varepsilon(E)$ for each composition for which $\varepsilon(E)$ is known. As these methods are not based on physical grounds it is not possible to predict $L(E)$ when a physical parameter, like temperature, is changed. A more physical approach expresses $L(E)$ with a finite sum of contributions of harmonic oscillators (HO). For instance, the room temperature $\varepsilon(E)$ of GaAs is fairly well described with seven oscillators [8]. The HO description is commonly used to describe $\varepsilon(E)$ of layers present at sample surfaces [9] or inside heterostructures [10]. The HO do not express the peculiarities of the optical response of a solid which appear at critical transitions. So the energies of the oscillators are not related to these transitions [11] and the different derivatives of L(E), so expressed, cannot reproduce those deduced from experimental data. The HO cannot describe correctly $\varepsilon(E)$ around the fundamental gap where $\varepsilon_i(E)$ has a sharp cut-off due to the strongly varying joint density of states.

Several model dielectric functions (MDF) have been proposed. Adachi describes $L(E)$ starting from the expression of $L_i(E)$ for parabolic bands above a critical point. $L_r(E)$ is then deduced analytically from a Kramers-Kronig inversion [12]. After such a calculation, the effect of the interactions with excitations in the crystal which broaden the transitions is phenomenologically introduced replacing E by $E + i\Gamma$ where Γ is a phenomenological broadening parameter associated with each critical

transition [13,14]. This model allows a fairly good description of $\varepsilon(E)$ but only if strong exciton contributions at critical points are introduced [15] or also large contributions from indirect transitions [16]. Recently, Kim *et al.* presented a still more elaborate MDF, though the expressions for $L(E)$ remain analytical [17]. This model rests on interpolation schemes, between critical points, of the parameters describing $L(E)$ around each of the critical transitions. The interpolations are done with polynomials limited to second order to obtain analytical expressions for the different parts of $L(E)$. All the necessary parameters entering these expressions are adjusted to obtain the best fit of $\varepsilon(E)$ but also of its two first derivatives. To date this model appears the most elaborate among those related to the physics governing $L(E)$. Owing to its numerous parameters it is able to model with great precision $\varepsilon(E)$ of binary compounds [17,18]. $\varepsilon(E)$ of $Ga_{1-x}Al_xAs$ has also been modelled by the same authors [19] using $\varepsilon(E)$ data for 8 selected compositions x and GaAs obtained mainly on layers which where grown by liquid phase epitaxy [20] in the same laboratory. The variations, with composition, of the parameters entering the expressions of $L(E)$ for a given x are then fitted with polynomials of cubic order whose coefficients are adjusted to give the best fit of $L(E)$ to $\varepsilon(E)$ data for all the selected compositions. $L(E)$ of GaAlAs can be then calculated, throughout the whole composition range, from a table of 84 coefficients independent of x. $L(E)$ reproduces fairly well $\varepsilon(E)$ data for $x < 0.8$.

This same model has been used, more recently, by Kamlet and Therry [21] for the case of InGaAsP quaternaries lattice matched to InP. Good results are obtained for each composition after fits to 58 parameters. However, the authors point out the paramount importance of the precise determination of the energies E_j and the broadening parameter Γ_j associated with each critical transition j. In a first step E_j and Γ_j are fitted with quadratic polynomials on composition. Then, the whole of the data is fitted anew using 176 parameters, all independent of composition. However, among all these parameters only fitted values of E_j are given for some selected compositions. The ability of $L(E)$ to describe the dielectric function is checked by determining the composition of some quaternaries used to evaluate $L(E)$. The study of a great number of examples show that the error on composition can reach 1%.

In this paper we present an attempt to model $\varepsilon(E)$ of the II-VI ternaries $Hg_{1-x}Zn_xTe$ (MZT_x) and $Cd_{1-x}Zn_xTe$ (CZT_x) with a discussion of the three models considered. We use the model of Kim *et al.* [17] changing slightly the paths of integration. Experimental data have been obtained in the same laboratory on good bulk samples. The paper is organized as follows: in Section 2 we recall shortly how experimental data have been acquired and the basis of the $L(E)$ description using different models. The third part focuses essentially on the fits with the model of Kim *et al.* [17] which is used to express $L(E)$ for each composition in HgZnTe and CdZnTe. Section 4 discusses the attempt to obtain a composition dependent model in both II-VI ternaries considered. Some comments on the potential accuracy of this modeling are presented as regard to the actual experimental situation. Section 5 gives briefly some comparisons with known results in the transparent domain of these semiconductors. The paper ends with the conclusion.

2 Experimental data and dielectric function models

$\varepsilon(E)$ has been deduced from ellipsometric measurements at room temperature between 0.75 and 5.6 eV. They were performed on good quality crystals grown by the traveling heater method. Experimental details are given with $\varepsilon(E)$ variations in reference [22] for MZT and in reference [23] for CZT. In these reports, $\varepsilon(E)$ is analyzed with the single critical point (SCP) model. The comparison between $L(E)$ given by the SCP model and $\varepsilon(E)$ is performed on their third derivatives [22,23]. The experimental acquisition of the optical data is equivalent to a mean of more than 10 measurements [22]. The noise in the data is then low enough to calculate the different derivatives and to obtain excellent fits of third derivatives of $\varepsilon(E)$ with those of $L(E)$ given by the SCP model. Only the fit around the weak $E_0 + \Delta_0$ transition is not so good. The different critical transitions have been discussed in [22] and [23]. E_1 and $E_1 + \Delta_1$ transitions can be equally well described by excitonic and or 2D transitions in both ternaries [22,23]. The three models used to describe $\varepsilon(E)$ are now discussed. Their basis is very briefly recalled; the details can be found in the references cited for each model.

In the first simple model considered $L(E)$ is expressed with a finite sum of harmonic oscillator (HO) contributions and written $L_{HO}(E)$:

$$L_{HO}(E) = L_{rHO}(E) + iL_{iHO}(E) = \varepsilon_1 + \sum_{j=1}^{N} A_j \left[\frac{1}{E - E_j + i\Gamma_j} - \frac{1}{E + E_j + i\Gamma_j}\right]$$

where E_j, Γ_j and A_j are respectively the energy, the broadening parameter, and the oscillator strength of oscillator j, ε_1 takes into account the effect of high energy transitions. $\varepsilon(E)$ is very well described in a large energy domain with only $N = 4$. This can be seen in Figure 1 where $L_{HO}(E)$ and $\varepsilon(E)$ are drawn for MZT 0.484. The corresponding E_j values are reported in Table 1 where they are placed arbitrarily in the same columns as those of real optical transitions for the sake of simplicity. In this fit 16 parameters have been adjusted. $\varepsilon_r(E)$ and $\varepsilon_i(E)$ are not correctly reproduced in the vicinity of the fundamental gap which is of crucial importance. Below the band gap, the absorption $L_{iHO}(E)$ is too high, $L_{rHO}(E)$ too low and its variations do not follow $\varepsilon_r(E)$ closer than 10%. The E_j are not related to the band structure so that $L_{HO}(E)$ derivatives should not be compared to those of $\varepsilon(E)$.

Table 1. Values of energies E_j, broadening parameters Γ_j giving a good fit of the dielectric function of MZT 0.484 with the oscillator model and the model of Adachi. The values deduced from the SCP model are recalled. Harmonic oscillator energies are arbitrarily placed in the table.

Model	E_0 (eV)	$E_0+\Delta_0$ (eV)	E_1 (eV)	$E_1+\Delta_1$ (eV)	E_2 (eV)	Γ_{E_0} (meV)	$\Gamma_{E_0+\Delta_0}$ (meV)	Γ_{E_1} (meV)	$\Gamma_{E_1+\Delta_1}$ (meV)	Γ_{E_2} (meV)
HO	–	2.546	3.135	4.691	6.818	–	227	711	913	4 012
MDF	0.890	–	2.543	2.961	4.871	30	–	355	101	317
SCP	0.850	1.720	2.557	3.239	4.678	58	47	139	193	165

Table 2. Critical transitions considered, their type and their connection with other critical points following the same bands in the Brillouin zone in HgZnTe and CdZnTe.

Critical Point	Transition	Type (3D)	Connexion to other Critical
$E_0(\Gamma)$	$(\Gamma_8^v \rightarrow \Gamma_6^c)$	M_0	E_1, $E_1+\Delta_1$, E_2
$E_0(\Gamma)+\Delta_0(\Gamma)$	$(\Gamma_7^v \rightarrow \Gamma_6^c)$	M_0	E_e
$E_1(\Lambda)$	$(L_{4,5}^v \rightarrow L_6^c)$	M_1	E_2
$E_1(\Lambda)+\Delta_1(\Lambda)$	$(L_6^v \rightarrow L_6^c)$	M_1	E_e
$E_2(X)$	$(X_7^v \rightarrow X_6^c)$	M_1	E_e

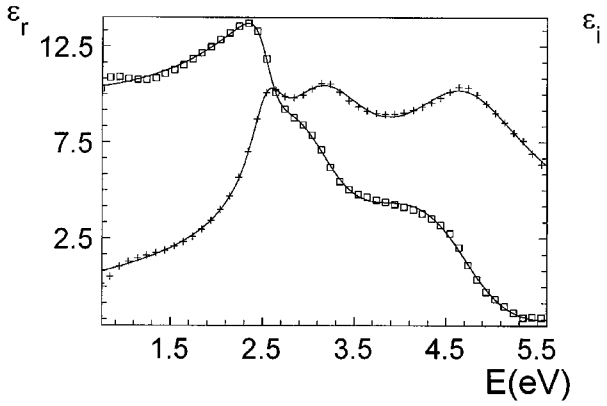

Fig. 1. Dielectric function of MZT 0.484 *versus* photon energy E: experimental data (□) ε_r, (+) ε_i, (——) description with 4 harmonic oscillators whose parameters are given in Table 1.

The MDF model is a great improvement in the modeling of $\varepsilon(E)$ as it links $L(E)$ to electronic transitions between bands. We will restrict discussion to the model proposed by Adachi [12]. The types of transitions corresponding to critical points are recalled in Table 2 as deduced from the SCP analysis [22,23]. The different necessary expressions are [12]:

$$L_{M_0}(E_j) = A_j E_j^{-3/2} \chi_j^{-2} \times \left[2 - (1+\chi_j)^{1/2} - (1-\chi_j)^{1/2} H(1-\chi_j)\right]$$

for a 3D M_0 transition at E_j.

$$L_{M_1}(E_j) = -B_j \chi_j^{-2} \ln(1-\chi_j)$$

for a 3D M_1 transition. In both expressions $\chi_j = (E + i\Gamma_j)/E_j$, A_j and B_j are oscillator strengths, Γ_j is the broadening parameter added after the analytic integration as explained in the introduction, and H is the Heaviside function. Strong excitonic contributions must be also added for the $\varepsilon(E)$ modeling. The usual expression of this type of contribution is:

$$L_{ex}(E_j) = \sum_{n-1}^{\infty} \frac{1}{(2n-1)^3} \left[\frac{C_j}{E_j - \dfrac{E_x}{(2n-1)^2} - E - i\Gamma_{ex}}\right]$$

where E_x is the binding energy of the exciton and Γ_{ex} the corresponding broadening parameter. In practice this sum is limited to $n=3$, and then $L(E)$ reads:

$$L_{MDF}(E) = \varepsilon_2 + L_{M_0}(E_0) + L_{M_0}(E_0+\Delta_0) + L_{M_1}(E_1) + L_{ex}(E_1) + L_{M_1}(E_1+\Delta_1) + L_{ex}(E_1+\Delta_1) + L_{M_1}(E_2)$$

as only five transitions have been found in MZT and CZT for the range of photon energies considered [22,23] (*cf.* Tab. 2). ε_2 describes the contribution of high energy transitions. These transitions are labeled with their usual name which are recalled in Table 2. $\varepsilon(E)$ can be well reproduced by this $L_{MDF}(E)$ at low energies when exciton contributions are ignored at E_0 and $E_0+\Delta_0$, though its importance increases with the fundamental gap E_0 [22,23]. Although the fit is performed simultaneously on $\varepsilon_r(E)$ and $\varepsilon_i(E)$ data, Figure 2 shows only the comparison of different choices in the modeling procedure, only on $\varepsilon_i(E)$. As already noticed, $L(E)$ cannot be adjusted to $\varepsilon(E)$ around E_1 and $E_1+\Delta_1$ transitions if excitonic contributions are not taken into account, even if all the parameters are taken free. When excitonic contributions are taken into account

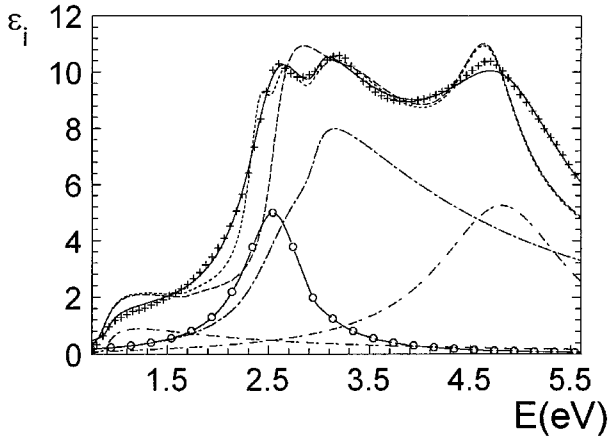

Fig. 2. Same $\varepsilon_i(E)$ as in Figure 1 for MZT 0.484: (+) experimental data, (- - -) best fit without excitonic contributions, (– –) fit after the introduction of excitonic contributions at E_1 and $E_1 + \Delta_1$ but taking the energies and broadenings deduced from the SCP model and given in Table 1. (——) Fit with excitonic contributions and taking all the parameters free. The four lower curves give the different contributions after the last fit. (—○—) Excitonic contribution at E_1 and $E_1 + \Delta_1$; (— - —) Other uncorrelated transitions.

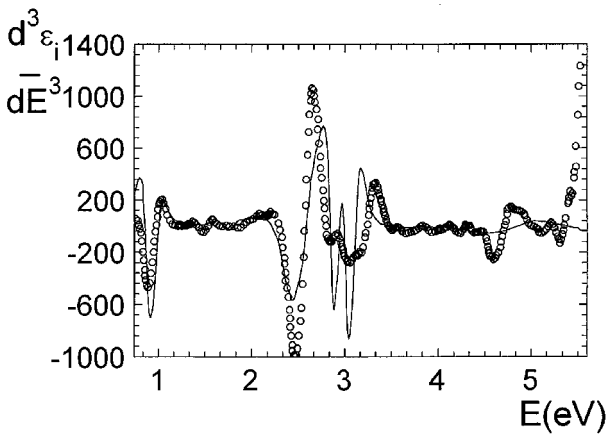

Fig. 3. Third derivative of $\varepsilon_i(E)$ for MZT 0.484 *versus* photon energy: (○) deduced from experimental data, (——) after the best fit with excitonic contributions.

$\varepsilon(E)$ is not correctly reproduced if the energies and broadening parameters are fixed at their values deduced from the SCP analysis [22,23] and given in Table 1. A good modeling is only achieved if all the 22 parameters entering $L_{MDF}(E)$ are taken free in the fit of $\varepsilon(E)$ data. Figure 2 displays also the different contributions corresponding to this fit and shows the large excitonic part introduced near E_1 and $E_1 + \Delta_1$. This large excitonic contribution disagrees with the conclusions of the SCP analyses [22]. It appears more clearly unrealistic if the derivatives of $L(E)$ and $\varepsilon(E)$ are compared. The oscillations in $d^3L_i(E)/dE^3$ shown in Figure 3 above E_1 are due to the excitonic part and are not present in $\varepsilon_i(E)$ when the amplitude of the doublet at E_1 appears too low. Attempts to obtain a simultaneous fit of $\varepsilon(E)$ and its two first derivatives have not been successful as can be guessed by the inspection of Figure 2 for the different types of fit. The energies of all critical transitions, which are reported in Table 1, appear appreciably shifted to higher energies due to the too high excitonic contribution.

The model of Kim *et al.* [17] is of the MDF type. However the broadening of the transitions is introduced before the integration of their polarizability contributions. The usual expression of the dielectric response of an isotropic medium in the Lorentzian approximation is [17].

$$L(E) = 1 - \lim_{\Gamma \to 0} \frac{8\pi^2 e^2}{m^2} \sum_{C,V} \int \frac{P_{CV}^2(E') J_{CV}(E')}{E'^2} \times \left[\frac{1}{E - E' + i\Gamma(E')} - \frac{1}{E + E' + i\Gamma(E')} \right] dE' \quad (1)$$

$P_{CV}(E')$ is the average of the momentum operator calculated over the surface of constant energy E' in the Brillouin zone. $J_{CV}(E')$ is the corresponding joint density of states and m the rest mass of the electron. The assumption of constant $P_{CV}(E')$ and parabolic bands leads to the usual expression of $L(E)$ of the SCP model [25] or first MDF model [12]. Kim *et al.* [17] interpolate the product $P_{CV}^2(E')J_{CV}(E') = W(E')$ between the expressions corresponding to the usual and simple description of two critical transitions. This interpolation uses polynomials noted p_j and q_j which multiply the strong variation of the joint density of states around critical points.

The polynomials take into account the non parabolicity of the bands and the variation of $P_{CV}(E')$. Following the interband transitions between critical points whose name and type are given in Table 2, the expressions of $W(E')$ take the forms [17]

$$W^{(E')}_{E_0 \to E_1} = p_1(E')\sqrt{E' - E_0} - q_1(E')\sqrt{E' - E_0}\sqrt{E_1 - E'} \quad (2)$$

$$W^{(E')}_{E_1 \to E_2} = p_2(E') - q_2(E')\sqrt{E_2 - E'} \quad (3)$$

$$W^{(E')}_{E_2 \to E_e} = p_3(E') - q_3(E')\sqrt{E' - E_2} \quad (4)$$

$$W^{(E')}_{E_0 \to E_2} = p_4(E')\sqrt{E' - E_0} - q_4(E')\sqrt{E' - E_0}\sqrt{E_2 - E'} \quad (5)$$

$$W^{(E')}_{E_0 \to E_1 + \Delta_1} = p_5(E')\sqrt{E' - E_0} - q_5(E')\sqrt{E' - E_0}\sqrt{E_1 + \Delta_1 - E'} \quad (6)$$

$$W^{(E')}_{E_1 + \Delta_1 \to E_e} = p_6(E') \quad (7)$$

$$W^{(E')}_{E_0 + \Delta_0 \to E_e} = p_7(E')\sqrt{E' - (E_0 + \Delta_0)}. \quad (8)$$

The upper energy E_e is, in fact, self contained in the values of the coefficients of the corresponding polynomials. The interpolations given here between critical points follow the transitions between filled and empty bands in the Brillouin zone and are given in Table 2. They are not completely the same as those chosen in reference [17], but this has no consequence on the fit of $\varepsilon(E)$ as the interpolation polynomials are not related to specific features of the band structure.

The $W(E')$ given by (2–8) are put in (1), and the broadening parameter $\Gamma(E')$ is, somewhat arbitrarily, interpolated between its values Γ_i and Γ_f at the lower (E_i)

and upper limits (E_f) of each of the integrals which are also one of the critical points given in (2–8).

$$\Gamma(E') = \gamma E + \beta \tag{9}$$
$$\text{where} \quad \gamma = \frac{\Gamma_f - \Gamma_i}{E_f - E_i} \quad \text{and} \quad \beta = \frac{E_f\Gamma_i - E_i\Gamma_f}{E_f - E_i}\,.$$

The integrals can thus be performed analytically and $L(E)$ reads then:

$$\begin{aligned} L(E) = 1 - \frac{8\pi\hbar^2e^2}{m^2}\sum_{n=0}^{2} & \left[p_{1n}H_n(E) - q_{1n}F_n(E)\right]_{E_0\to E_1} \\ & + \left[p_{2n}G_n(E) - q_{2n}K_n(E)\right]_{E_1\to E_2} \\ & + \left[p_{3n}G_n(E) - q_{3n}H_n(E)\right]_{E_2\to E_e} \\ & + \left[p_{4n}H_n(E) - q_{4n}F_n(E)\right]_{E_0\to E_2} \\ & + \left[p_{5n}H_n(E) - q_{5n}F_n(E)\right]_{E_0\to E_1+\Delta_1} \\ & + \left[p_{6n}G_n(E)\right]_{E_1+\Delta_1\to E_e} \\ & + \left[p_{7n}H_n(E)\right]_{E_0+\Delta_0\to E_e} + r_{00}. \end{aligned} \tag{10}$$

Where $p_{in}(q_{in})$ is the coefficient of $(E')^n$ in $p_i(E')(q_i(E'))$. $F_n(E)$, $G_n(E)$, $H_n(E)$ and $K_n(E)$ are integrals whose analytic expressions are given in the appendix of reference [17] and in [26]. Integral limits E_i and E_f are given in (10) by lower indices at the right of each bracket. The contribution of transitions of energy higher than E_e are simply expressed through the constant r_{00}. This contribution has been simulated by a polynomial in [17] which does not satisfy Kramers-Kronig relations and, better, by an harmonic oscillator [21]. However the model contains a great number of fitting parameters, here 47 for a Lorentzian broadening, and it appears more than enough to gather the small contribution of transitions above E_e in the constant r_{00}.

The effect of a Gaussian broadening near a critical point E_j can be fairly well introduced in $L(E)$ replacing the Lorentzian broadening Γ_j by

$$D_j = \Gamma_j e^{\alpha_j\left(\frac{E'-E_j}{\Gamma_j}\right)^2} \tag{11}$$

[17] where α_j is an adjustable parameter.

This change in some broadenings improves the fit of experimental data especially in the vicinity of the fundamental gap E_0 [17,18].

3 Fitting procedure and results for defined compositions

The main points of the discussion on the HO and the MDF model have been already given in Section 2. We want to emphasize that the simple HO model is adequate, if one is only interested in the knowledge of the composition in one of the two ternaries studied, as $\varepsilon(E)$ varies strongly with x. We found that the use of the HO model leads to a determination of x with an accuracy of 0.7% which is near the absolute uncertainty on the x determination. A slight improvement in x is reached when using the SCP model with the main critical transitions; however it needs more calculations and more attention in the evaluation of $\varepsilon(E)$ derivatives and their fit to the SCP model as the results depend on the type of critical transition chosen.

The Kim *et al.* modeling of $\varepsilon(E)$ needs the following steps: for each individual composition of a ternary where good experimental data have been obtained, $L(E)$ is fitted to $\varepsilon(E)$ with Lorentzian expressions of the broadenings. A Gaussian broadening is then introduced and its effect examined. For a given x, the individual fit is performed in two steps [17] as all the parameters do not have the same importance. In a first step, the energies and broadening parameters of the critical transitions are evaluated. Their values can be determined independently using the SCP model. We found that the E_j values deduced from the fit of the third derivatives of $\varepsilon_r(E)$ and $\varepsilon_i(E)$ with the SCP model are the same, within ± 4 meV as those deduced using directly the Kim *et al.* model. The deviations between both fits are within the uncertainties in the determination of these energies [22,23]. The deviations on the Γ_j using both models have also the same amplitude. This excellent agreement is found only when the type of critical transition chosen in the SCP model is the same as that used in the model of Kim *et al.* E_j and Γ_j values so deduced have been given for about 10 compositions in [22] for MZT and in [23] for CZT; they are given in Table 3.

In the second step the 37 other parameters entering (10) are adjusted using the Levenberg-Marquard method [27] so as to obtain the best fit on $\varepsilon(E)$. A global test of the convergence of the fit is given by the confidence parameter:

$$\chi^2 = \frac{1}{N-m}\sum_{i=1}^{N}\left\{\frac{\left[\varepsilon_r(E_i) - L_r(E_i)\right]^2}{\sigma_r^2} + \frac{\left[\varepsilon_i(E) - L_i(E)\right]^2}{\sigma_i^2}\right\} \tag{12}$$

N is the number of photon energies at which ε has been measured, m the number of parameters to be adjusted, σ_r^2 and σ_i^2 are experimental standard deviations on all the photon spectrum.

This two step procedure is more tedious to handle, however the determination of the E_j and Γ_j which describe $\varepsilon(E)$ variations very near critical transitions with the SCP model do not interact with those of the coefficients of the interpolation polynomials p_{in} and q_{in}. It avoids spurious convergences of some p_{in} or q_{in} around weak transitions such as $E_0 + \Delta_0$ [21]. In MZT, E_0 lies below the lowest photon energy of the experimental $\varepsilon(E)$ spectrum for $x < 0.45$: E_0 is then deduced from optical absorption measurements [28] and the p_{1n} and p_{7n} are adjusted in a last fit so as to obtain the low frequency dielectric constant deduced from infrared reflectivity data [29].

Good individual fits lead to a great number of p_{in} and q_{in} equal to zero [18,19,21]. We have not been able to define mathematical criterions stating what parameters are of small importance in a fit. However we found obvious general rules which are of great help during the fitting

Table 3. Energies E_j and broadening parameters Γ_j of critical transitions for the different compositions x considered in HgZnTe and CdZnTe as deduced from the SCP fit.

	$Hg_{1-x}Zn_xTe$										
x	0	0.106	0.148	0.216	0.294	0.424	0.484	0.640	0.814	0.920	1
E_0 (eV)	–	–	–	–	–	–	0.850	1.256	1.686	2.011	2.273
Γ_0 (meV)	–	–	–	–	–	–	58	46	36	17	10
$E_0+\Delta_0$ (eV)	–	–	0.798	1.124	1.394	1.544	1.720	2.187	2.584	–	3.193
$\Gamma_{E_0+\Delta_0}$ (meV)	–	–	1	2	37	57	47	53	66	–	3
E_1 (eV)	2.109	2.216	2.245	2.273	2.399	2.525	2.557	2.820	3.125	3.463	3.632
Γ_{E_1} (meV)	65	85	101	108	114	125	139	126	88	80	68
$E_1+\Delta_1$ (eV)	2.753	2.862	2.899	2.927	3.063	3.180	3.239	3.499	3.789	4.018	4.226
$\Gamma_{E_1+\Delta_1}$ (meV)	79	142	144	159	156	186	193	165	160	144	96
E_2 (eV)	4.337	4.451	4.445	4.498	4.557	4.632	4.678	4.863	5.014	5.232	5.280
Γ_{E_2} (meV)	371	334	269	245	203	161	165	95	120	180	183

	$Cd_{1-x}Zn_xTe$								
x	0	0.052	0.180	0.260	0.410	0.512	0.616	0.872	1
E_0 (eV)	1.518	1.534	1.615	1.66	1.762	1.847	1.922	2.139	2.273
Γ_0 (meV)	12	13	12	8	10	12	12	7	10
$E_0+\Delta_0$ (eV)	2.452	2.471	2.541	2.578	2.72	2.783	2.832	3.094	3.193
$\Gamma_{E_0+\Delta_0}$ (meV)	37	59	7	51	22	25	43	54	3
E_1 (eV)	3.623	3.369	3.383	3.381	3.41	3.433	3.481	3.573	3.632
Γ_{E_1} (meV)	60	73	72	76	79	85	82	73	68
$E_1+\Delta_1$ (eV)	3.96	3.966	3.98	3.981	4.017	4.053	4.095	4.15	4.226
$\Gamma_{E_1+\Delta_1}$ (meV)	110	113	115	108	126	128	142	103	96
E_2 (eV)	5.04	5.011	4.945	4.986	5.065	5.154	5.201	5.268	5.28
Γ_{E_2} (meV)	197	232	231	204	223	200	202	170	183

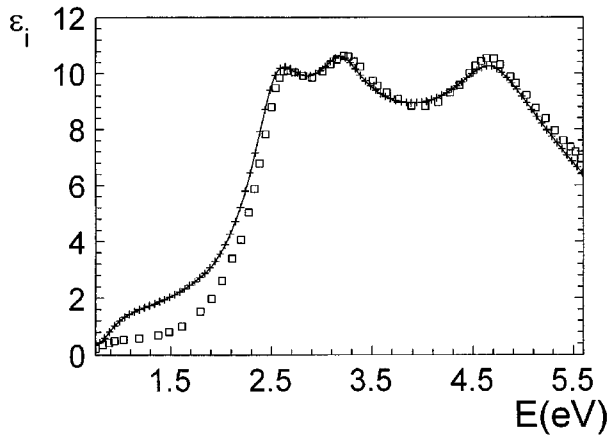

Fig. 4. $\varepsilon_i(E)$ of MZT 0.484: (+) experimental data, (—) after the individual fit with the model of Kim *et al.*, (□) after adjustment of the parameters of the composition dependent model.

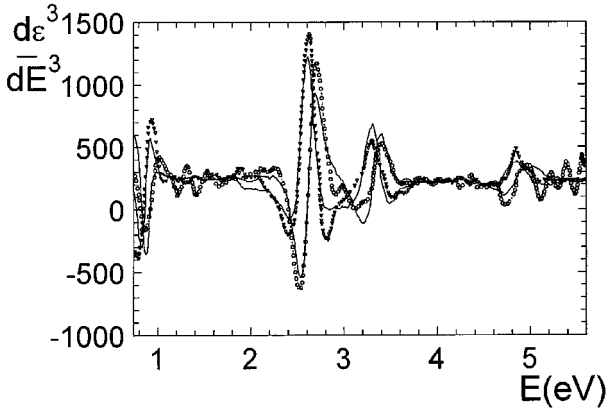

Fig. 5. Third derivatives of $\varepsilon_r(E)$ and $\varepsilon_i(E)$: (∇)ε_r, (○)ε_i as deduced from experimental data, (—) after the individual fit with the model of Kim *et al.*

procedure. The higher the order of an interpolation polynomial the less easy is the convergence of the fit with larger deviations between $L(E)$ and $\varepsilon(E)$. The influence of an interpolation polynomial between two critical transitions decreases when the photon energy goes far from these transitions. This allows the limiting of the order of the polynomials to zero for high energy transitions [18]. In each of the seven brackets of (10), the contribution of the p_{jn} is important in the lower half interval of integration between E_i and E_f. In return the q_{jn} contributes mainly in the higher half interval. In fact both p_{in} and q_{in} are adjusted so as to obtain the smallest difference between $L(E)$ and $\varepsilon(E)$ in the middle of $E_f - E_i$. Very near a critical point $\varepsilon(E)$ is very well modelled with constant terms (p_{io} or q_{io}) in agreement with the accuracy of the SCP model. We have been able to obtain good fits for each composition in MZT and CZT with only 15 non-zero parameters with a confidence parameter usually lower than 1. As an example, $\varepsilon(E)$ and $L(E)$ are compared

in Figure 4 and their third derivatives in Figure 5 for MZT 0.484. They show that such a model is the most accurate as it describes well the behaviour of $\varepsilon(E)$ both around critical transitions and between these transitions.

The largest deviations of $L(E)$ from $\varepsilon(E)$ remain, however, on $\varepsilon_i(E)$ just below the fundamental gap. A Gaussian broadening introduced in the three transitions of lowest energy has not improved the fit in a convincing way. For the sake of comparison an enlargement of the spectral region around E_0 of the results of the model of Kim *et al.* for CdTe is reproduced in Figure 6 with our results. We see in this figure that the Lorentzian fit of our measured $\varepsilon_r(E)$ is very good and our $L_r(E)$ variations below E_0 are as good as those given by Kim *et al.* [18]. In return our $\varepsilon_i(E)$ variations deduced with the Lorentzian fit are not the same. If the fit is not very good below E_0 it appears better above the fundamental gap. Fits with a Gaussian description may improve $\varepsilon_i(E)$ below E_0 but to the detriment of the part above the gap and of $\varepsilon_r(E)$ below the gap. As the Gaussian description adds another adjustable parameter we prefer to keep the Lorentzian one to start the last step of the modeling procedure.

4 Composition dependent model and discussion

The working out of a composition-dependent model needs to describe the variations, with x, of each of the parameters of the model. The $E_j(x)$ variations are well reproduced by second order polynomials as the difference between their actual value and the linear interpolation between the value corresponding to the end binaries is almost symmetric as referred to $x = 0.5$ [22]. The Γ_j must also have smooth variations with x and are tentatively described by second order, but also third order polynomials. One expects also smooth variations with x for all the other coefficients of the polynomials entering (10). This global modeling appears relatively bad despite the high order of the polynomials used to describe the x variations of these coefficients. This is even more obvious for the chosen example of MZT 0.484. $\varepsilon_i(E)$ is also shown in Figure 4 after one of the best global fits. The description is clearly rather bad as compared to the individual fit for this composition. Table 4 gives the values of the p_{in} and q_{in} obtained for this composition after the global fit which have to be compared with those obtained after the individual fit of $\varepsilon(E)$ which are given in the next row. Table 4 gives also the order s of the fitting polynomials and the relative deviation δ on the 15 parameters used for the individual fits. $L(E)$ appears to be very sensitive to the value of p_{in} and q_{in}. A relative change of 1% in one of these parameters can lead to a change of more than 10% in $\varepsilon_i(E)$ between the energies of the critical transitions where it has the greatest effect. An analysis of the origin of the failure of a good global fit shows that it comes mainly from the deviations of the values of the Γ_j from a smooth curve describing their x variations. This can be seen clearly by inspection of Figure 8 of [22] and Figure 5 of [23]. One way to obtain a better global fit is obviously to describe $\Gamma_j(x)$ variations with a polynomial of high order. In fact the model is improved with $\Gamma_j(x)$ described with polynomials the orders of which are the same as the number of compositions for which $L(E)$ has been fitted to $\varepsilon(E)$ that is 10 for MZT and 8 for CZT. However, this type of description does not rest on any physical ground but try to take into account the uncertainties arising in the measurements.

The experimental uncertainties on the determinations of $\varepsilon_r(E)$ and $\varepsilon_i(E)$ are now smaller than 0.5% with existing ellipsometers. This is seen in the error bars of the energies of the critical transitions which remain lower than 10^{-2} [18,22,23]. A systematic error comes from the presence of an overlayer on the surface of bulk samples after chemical treatments which give the "best" results [2, 4,22,23]. However, if the overlayer cannot be completely eliminated, it can be controlled through different tests. Moreover the final contribution of the overlayer to the deviations of $\varepsilon(E)$ as compared to the actual value can have only a smooth variation on composition. Depolarisation effects originating from the roughness of sample surfaces lead also to deviations on $\varepsilon(E)$ from its actual bulk value. This roughness is optically equivalent to an overlayer which must be added to the one previously discussed. Inspection of the surfaces by atomic force microscopy show that their roughness remains weak and almost independent of x in both ternaries after the best chemical treatments [22,23]. The root mean square roughness increases slightly from 0.38 nm for CdTe to 0.64 nm for HgTe and 0.65 nm for ZnTe [30]. So the depolarisation effects remain weak and should vary smoothly with x.

The main origin of the uncertainty in Γ_j rests on the elaboration of the bulk materials. The E_j but especially the Γ_j change with doping [31,32]. In GaAs [32] the changes are greater for n-type doping than for p-type doping and depends on the type of dopant. The problem is not simple as the effect on the lattice differs from one dopant to the other. The residual doping of the measured samples is lower than 10^{16} cm^{-3} in CZT and MZT with $x > 0.6$ and lower than 10^{17} cm^{-3} in MZT with $x < 0.6$. These limited dopings lead, at most, to Γ_j increases of 10 meV. These changes are non-negligible as compared to Γ_j values which stay in the 100 meV range. Actually, all the defects contribute, more or less, to the E_j and Γ_j changes and we have no precise knowledge of their concentrations. Extended defects contribute, in addition, to the lattice polarizability and to the Γ_j. Deviations from stoichiometry are large in tellurium based II-VI compounds leading to Te precipitates after low temperature annealings under a controlled pressure of one of the cation components [33–35]. Te precipitates have a non-negligible contribution to the polarizability and also probably to the Γ_j. It has been shown [36] that the commonly assumed value of the dielectric constant, at 10.6 nm of 7.28 for ZnTe [37] can be lowered to $\varepsilon_r = 6.75$ after a very long annealing in liquid Zn. The concentrations of the different defects is difficult to control and even to measure in bulk semiconductors. The main part of the erratic deviations of the Γ_j from

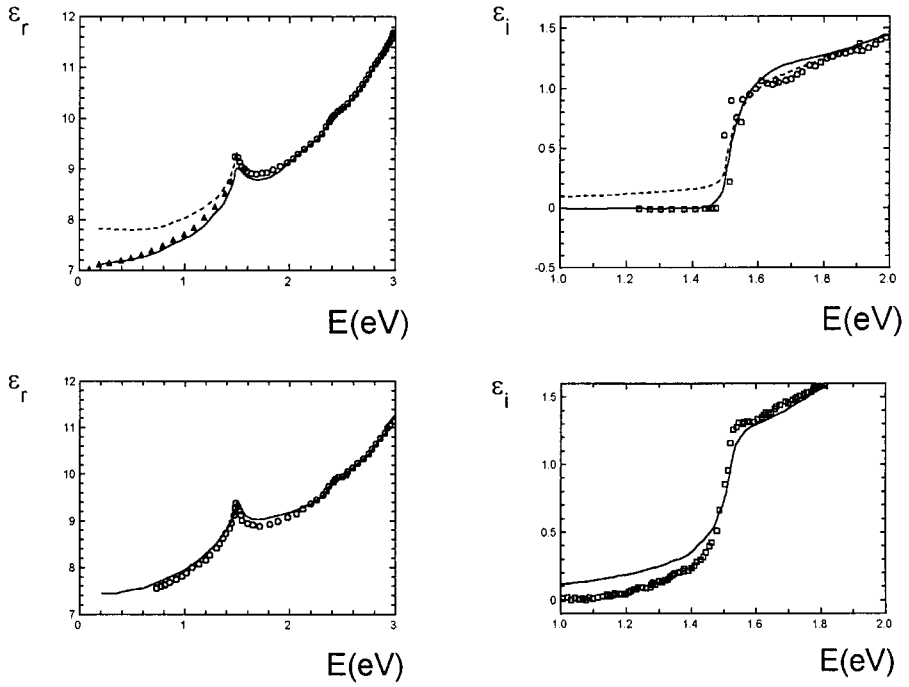

Fig. 6. Enlargement of the spectral domain near Eo of CdTe: (a) $\varepsilon_r(E)$ and $\varepsilon_i(E)$ reproduced from [18], $(\triangle, \circ)\,\varepsilon_r$, $(\square, \circ)\,\varepsilon_i$ experimental data, (- - -) Lorentzian fit, (——) Gaussian fit. (b) Our experimental results, $(\circ)\,\varepsilon_r$, $(\square)\,\varepsilon_i$, (——) Lorentzian fit.

Table 4. Value of the coefficients entering (10) after the global fit (GF) to obtain a composition dependent model for MZT 0.484 which are to be compared to their values after the individual fit (IF) on experimental results for this composition; s is the order of the fitting polynomial and δ the relative deviation on the coefficients.

	$p_{1,0}$	$p_{1,1}$	$q_{1,0}$	$q_{1,1}$	$p_{7,0}$	$p_{2,0}$	$p_{2,1}$	$q_{2,0}$	$q_{5,0}$	$q_{5,1}$	$q_{4,0}$	$p_{6,0}$	$p_{3,0}$	$q_{3,1}$	$r_{0,0}$
GF	200	−51	188	−37	−1	239	−4.2	110	89	−4.6	66	23	76	4.7	0.9
IF	202	−52	189	−38	0	239	−3.9	109	89	−1.2	66	20	77	4.4	1.09
s	9	9	9	9	5	9	9	9	8	8	8	7	8	8	7
δ	0.005	0.02	0.005	0.03	0.1	$< 10^{-3}$	0.08	0.01	$< 10^{-3}$	0.4	$< 10^{-3}$	0.15	0.01	0.07	0.2

smooth variations with x originates most probably from the unknown defect concentrations.

Another origin of erratic deviations in Γ_j may come from those of the composition of the samples used to measure $\varepsilon(E)$. Only samples where the estimated x variation on the tested area was less than 2×10^{-3} were measured. Such spreads in x lead to Γ_j enlargements with upper bounds of 3 meV for E_0 and $E_0 + \Delta_0$, and 1 meV for the other critical transitions in MZT; these are two times lower in CZT. These Γ_j increases represent about one tenth of the erratic deviations found on the Γ_j of MZT 0.484 already considered here. It appears most likely that non controlled defects in the bulk samples hinder a good global modeling of $\varepsilon(E)$ in the two II-VI ternaries studied. There is no comprehensive optical studies of these II-VI compounds when they are grown by epitaxial techniques. Some of these techniques allow a good control of purity and defects during the growth. This appears to be the case for some III-V alloys grown by molecular beam epitaxy for which $\varepsilon(E)$ data can be well described by the Kim *et al.* model in large composition domains [19,21].

5 ε predictions in the infrared and comparisons

Expression (10) allows the evaluation of $L(E)$ at frequencies below the fundamental gap but above the reststrahlen band due to lattice vibrations. $L_r(0)$ at zero frequency, calculated with (10) is called the dielectric constant ε_∞. $L_r(E)$ is calculated using the parameters deduced from the individual fits. The comparison of $L_r(0)$ with ε_∞ obtained on samples of the same source as those used for ellipsometric measurements [29] is given in Figure 7. These results are rather far from other experimental results obtained on bulk MZT grown by another method [38]. The strong variation of $\varepsilon_r(E)$ in MZT hides the small deviations due to different defect concentrations in samples of different

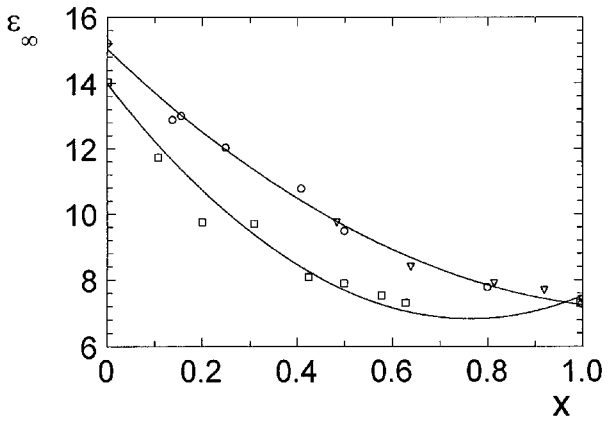

Fig. 7. Infra-red dielectric constant above phonon frequencies ε_∞ *versus* composition x in HgZnTe. (∇) calculated values after the fit with the model of Kim *et al.* on individual compositions, ($\circ$) from [29], ($\square$) from [38], lines give quadratic fits.

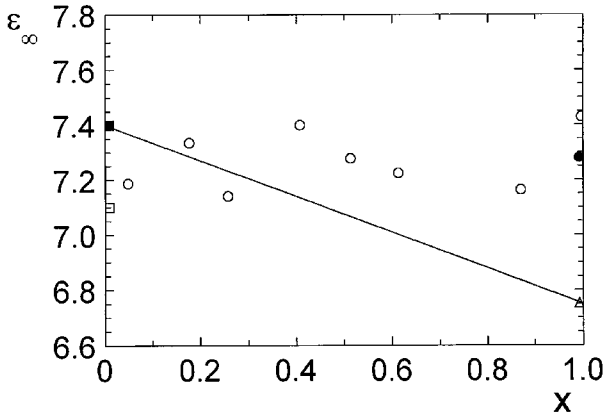

Fig. 8. Infra-red dielectric constant above phonon frequencies ε_∞ *versus* composition x in CdZnTe. ($\circ$) calculated values after the fit with the model of Kim *et al.* on individual compositions, ($\blacksquare$) from [39], ($\square$) from [41], ($\triangle$) from [42], ($\bullet$) from [36].

compositions. In return, the deviations of the calculated $L_r(0)$ from a smooth curve are clearly seen in the case of CZT as ε_∞ has a small variation with x. Figure 8 shows $\varepsilon_\infty = L_r(0)$ for compositions where $\varepsilon(E)$ have been measured. Values given in the literature for the end binaries are also reported. ε_∞ values of the ternaries are enclosed between those given for the binaries, for which the deviations should be attributed mainly to differences in defect concentrations of the samples rather that uncertainties on optical measurements. We see that, in the Cd rich side, where Zn increases the bond strength of CdTe, ε_∞ values are lower than 7.4 [39] which is the commonly considered value. ε_∞ of defect free CdTe is more likely near 7.2 [40] or 7.1 [41]. Zn rich compounds have ε_∞ higher than the value which can be interpolated between those of CdTe (7.2) and ZnTe (6.75). Zn rich CZT have probably higher defects concentrations which are more likely tellurium precipitates.

6 Conclusion

Among the three models considered for expressing the dielectric function of semiconductors, that of Kim *et al.* appears the most complete and powerful. The analytic interpolation of the product of the density of states and the matrix element of the transitions between critical transitions allows the description of $\varepsilon(E)$ both near critical points and between them with a great accuracy. This $\varepsilon(E)$ modeling remains a little heavy and should be used only if precise $\varepsilon(E)$ values are needed. The knowledge of parameters like composition x with an accuracy better than 1% is reached with simpler models like the harmonic oscillator one which is purely phenomenological.

In the case of the II-VI compounds considered we have failed in the elaboration of a precise composition dependent model. The lack of accuracy is not due to the model itself but rests on the metallurgical definition of the samples. The low composition inhomogeneity of the samples contributes but not to a great extent. The main part of the erratic deviations of the parameters of the model from a smooth variation with composition appear to originate from the densities of defects which are difficult to control during the growth and the following annealing treatments.

V. Drouot is gratefully acknowledged for the reading of the manuscript.

References

1. A. Yariv, *Optical Electronics, Series in Electrical Engineering* 4th ed., (Saunders Colleg. Publishing 1991).
2. P. Lautenschlager, M. Garriga, L. Viña, M. Cardona, Phys. Rev. B **36**, 4821 (1987).
3. P. Lautenschlager, M. Garriga, S. Logetheditis, M. Cardona, Phys. Rev. B **35**, 9174 (1987).
4. P. Lautenschlager, M. Garriga, M. Cardona, Phys. Rev. B **36**, 4613 (1987).
5. D.E. Aspnes, S.M. Kelso, R.A. Logan, R. Bhat, J. Appl. Phys. **60**, 754 (1986).
6. P.G. Snyder, J. Wollam, S.A. Alterovitz, B. Johs, J. Appl. Phys. **68**, 5925 (1990).
7. J.L. Freeouf, Appl. Phys. Lett. **53**, 2426 (1988).
8. M. Erman, J.B. Theeten, N. Vodjdani, Y. Demay, J. Vac. Sci. Technol. B **1**, 328 (1983).
9. D.E. Aspnes, G.P. Schwartz, G.J. Gualtieri, B. Schwartz, J. Electrochem. Soc. **128**, 590 (1981).
10. C.M. Herzinger, P.G. Snyder, F.G. Celii, Y.C. Kao, D. Chow, B. Johs, J.A. Woollam, J. Appl. Phys. **79**, 2663 (1996).
11. G.N. Maracas, G.H. Kus, S. Arnaud, R. Droopad, J. Appl. Phys. **77**, 1701 (1995).
12. S. Adachi, Phys. Rev. B **41**, 1003, references therein (1990).
13. F. Bassani, G. Pastori Parravicini, *Electronic States and Optical transitions in Solids* (Pergamon New-York 1975).

14. D.W. Jenkins, J. Appl. Phys. **68**, 1848 (1990).
15. S. Adachi, T. Taguchi, Phys. Rev. B **43**, 9569 (1991).
16. S. Adachi, Phys. Rev. B **35**, 7454 (1987).
17. C.C. Kim, J.W. Garland, H. Abad, P.M. Raccah, Phys. Rev. B **45**, 11749 (1992).
18. C.C. Kim, S. Sivananthan, J. Appl. Phys. **78**, 4003 (1995).
19. C.C. Kim, J.W. Garland, P.M. Raccah, Phys. Rev. B **47**, 1876 (1993).
20. D.E. Aspnes, S.M. Kelso, R.A. Logan, R. Bhat, J. Appl. Phys. **60**, 754 (1986).
21. L.I. Kamlet, F.L. Terry, Jr, J. Elect. Mat. **24**, 2005 (1995).
22. O. Castaing, J.T. Benhlal, R. Granger, R. Triboulet, J. Phys. I France **6**, 907 (1996).
23. O. Castaing, R. Granger, J.T. Benhlal, R. Triboulet, J. Phys. Cond. **81**, 5757 (1996).
24. H. Ehrenreich, M.H. Cohen, Phys. Rev. **115**, 286 (1959).
25. D.E. Aspnes in *Handbook on Semiconductors*, edited by M. Balkanski (North Holland Amsterdam, 1980) Vol. 2.
26. In the expression of $H_1(E)$, the sign before the second franction is $-$ in place of $+$. C. Kim point out to us this error which is also noted in reference [21].
27. W.H. Press, B.P. Flannery, S.A. Tenkolsky, W.T. Vetterling, *Numerical Recipes, the Art of Scientific computing* (Cambridge University Press 1989), p. 523.
28. B. Toulouse, R. Granger, S. Rolland, R. Triboulet, J. Phys. France **48**, 247 (1987).
29. G. Le Bastard, R. Granger, S. Rolland, Y. Marqueton, R. Triboulet, J. Phys. France **50**, 3223 (1989).
30. O. Castaing, thesis dissertation, INSA Rennes, 1997.
31. P.G. Snyder, Y.M. Xiong, Surf. Interf. Anal. **18**, 107 (1992).
32. F. Lukes, S. Gopalan, M. Cardona, Phys. Rev. B **47**, 7071 (1993).
33. P. Capper in *Narrow gap Cadmium based compounds* EMIS data rev. n° 10. (P. Caper Edit. London 1994), p. 489.
34. J.H. Tregilgas in *Narrow gap Cadmium based compounds* EMIS data rev. n° 10. (P. Caper Edit. London 1994), p. 185.
35. A. Lasbley, A. Seyni, C. Pelletier, R. Granger, R. Triboulet, Phys. Status Solidi **123**, 227 (1991).
36. A. Azena, P. Gaucherel, J.C. Ronstan, R. Granger, R. Triboulet, J. Appl. Phys. **68**, 6029 (1990).
37. G. Nimtz in *Landolt-Börnstein*, (Springer Verlag, Berlin, 1982) Vol. 17 p. 160.
38. M.P. Voltz, F.R. Szofran, S.L. Lehoczky, C.-H. Su, Solid State Commun. **75**, 943 (1990).
39. J. Baars, F. Sorger, Solid State Commun. **10**, 875 (1972).
40. M. Gorska, W. Nazarewicz, Phys. Status Solidi b **65**, 193 (1974).
41. A. Manabe, A. Mitsuishi, H. Yoshinaga, Jpn. J. Appl. Phys. **6**, 593 (1967).
42. D.T.F. Marple, J. Appl. Phys. **35**, 539 (1964).